Resilient Cities and Structures 3 (2024) 20–27

Contents lists available at ScienceDirect

Resilient Cities and Structures

journal homepage: www.elsevier.com/locate/rcns

Full Length Article

Upcrossing-based time-dependent resilience of aging structures

Cao Wang

School of Civil and Environmental Engineering, University of Technology Sydney, Ultimo, NSW 2007, Australia

ARTICLE INFO

Keywords:
Time-dependent resilience
Stochastic load process
Multiple damage states
Upcrossing
Closed form solution

ABSTRACT

The time-dependent resilience of an in-service aging structure provides quantitative measure of the structural ability to prepare for, adapt to, withstand and recover from disruptive events. Resilience models have been proposed in the literature to evaluate the resilience of aging structures subjected to discrete load processes, which are, however, not applicable to handle resilience problems considering continuous load processes. In this paper, a new method is developed to evaluate the time-dependent resilience of aging structures subjected to a continuous load process. The proposed method serves as the complement of the existing resilience models addressing discrete load processes, and takes into account the aging effects of the structural resistance/capacity and the nonstationarity in loads as a result of climate change. A structure suffers from a damage state upon the occurrence of an upcrossing of the load effect with respect to the resistance/capacity, leading to the reduction of the performance function, followed by a recovery process that restores the performance. The proposed method enables the time-dependent resilience to be evaluated via a closed form solution. It is also revealed that, the proposed resilience model takes an extended form of the existing formula for upcrossing-based time-dependent reliability, thus establishing a unified framework for the two quantities. The applicability of the proposed method is demonstrated through examining the time-dependent resilience of a residential building subjected to wind load. The effects of key factors on resilience, including the nonstationarity and correlation structure of the load process, as well as the resistance/capacity deterioration scenario, are investigated through an example. In particular, the structural resilience would be overestimated if ignoring the potential impacts of climate change, which is a relatively non-conservative evaluation.

1. Introduction

In-service engineering structures (e.g., bridges, and power plants) are expected to provide sufficient serviceability during their service lives, physically supporting modern societies' functionalities. However, these structures often suffer from the degradation of properties (e.g., strength, and stiffness) triggered by aggressive environmental attacks [1–4]. It is usually difficult or even impossible to predict the structural serviceability over a future service period in a deterministic manner, due to the uncertainties arising from the structural properties and external load effects. In this context, *reliability* and *resilience* have been two powerful indicators to measure structural serviceability in a probabilistic sense. The former evaluates the occurrence probability of a limit state (e.g., the load effect does not exceed the resistance) being violated [5,6], while the later (resilience) refers to the structural ability to prepare for, adapt to, withstand and recover from disruptive events [7,8]. In particular, the two quantities – reliability and resilience – are dependent on the time period of interest, and thus are known as time-dependent reliability and time-dependent resilience accordingly to reflect such dependence (In this paper, the term "time-dependent" refers to the dependence of a quantity on a *time interval*, which is distinguished from the term "time-variant" emphasizing the instantaneous variation of a quantity with time).

There are many types of load processes that can be modeled by a continuous stochastic process[1], which is the focus of this paper. Due to the potential impacts of climate change [10], the load process may display nonstationary characteristics (e.g., an increasing trend of intensity), which should be incorporated in the assessment of structural serviceability. For example, the increased likelihood of extreme waves as a result of sea level rise in a changing climate has been projected in recent studies [11–13]. In terms of future winds, it was shown in [14] that, structures at the East Coast of Australia may experience higher gust hazard compared with the design values as a result of climate change.

The evaluation methods for reliability have been relatively well documented in the literature. In [15], a closed form solution was derived for the time-dependent reliability assessment of aging structures subjected to a Gaussian load process. In the presence of other (general) types of load stochastic processes, Wang et al. [16] extended the Nataf transformation method, which was initially developed for discrete cor-

[1] More precisely, this paper considers quadratic mean continuous processes (QMCP), defined as follows (see definition in, e.g., [9]). For a second-order process $\{S(t)\}$, if the mean value of $[S(t_0+h)-S(t_0)]^2$ evaluated at any time t_0 approaches 0 as $h \to 0$, then $S(t)$ is deemed as a QMCP.

E-mail address: cao.wang@uts.edu.au

https://doi.org/10.1016/j.rcns.2024.05.001
Received 12 February 2024; Received in revised form 22 April 2024; Accepted 16 May 2024
Available online 27 May 2024

related random variables, to convert the non-Gaussian load process to a Gaussian one, with which the original reliability solution [15] becomes applicable. Other types of transformation methods (e.g., [17]) have also been applied to convert non-Gaussian load processes. Compared with the reliability methods, the resilience assessment of a structure additionally takes into account the post-hazard recovery process of structural performance. In [18], the time-dependent resilience of an aging structure was quantified through the accumulative performance losses to lifetime hazards, employing a renewal-reward process to model the time-variation of performance. In [19], the time-dependent resilience for aging structures in the presence of a discrete load process was studied. This work was later generalized in [20] to account for the effect of multiple post-hazard damage states on resilience. However, these models are not applicable when considering a continuous load process.

In this paper, a new method is developed to evaluate the time-dependent resilience of an aging structure subjected to a continuous load process, taking into account the impacts of climate change and the time-variation of structural resistance/capacity. The occurrence of an upcrossing (i.e., the load effect exceeds the resistance/capacity) results in structural damage/failure state, followed by a recovery process of structural performance. This yields a closed form solution for structural time-dependent resilience, which takes a generalized form of time-dependent reliability. An illustrative example is presented in this paper to demonstrate the applicability of the proposed resilience method. The effects of key affecting factors on resilience are investigated through sensitivity analysis. In particular, it is demonstrated that, if ignoring the potential impacts of climate change, the resilience will be underestimated, which is a nonconservative evaluation of structural serviceability.

2. Upcrossing-based time-dependent reliability

In this section, the assessment method for time-dependent reliability is reviewed. This serves as a basis for the further comparison between reliability and resilience, as will be addressed in the next section.

Consider the reliability of an aging structure over a reference period of $[0, t_l]$ subjected to a stochastic load process $S(t)$. As shown in Fig. 1(a), let $r(t)$ be the time-variant resistance at time t, which degrades with time as a result of external environmental attacks. Here, $r(t)$ is a deterministic process, written in a lower case, whose uncertainty will be addressed later. The time-variation of resistance can be modeled by a deterioration function $g(t)$ [21], i.e., $r(t) = r(0) \cdot g(t)$. An "upcrossing" is deemed to occur if $S(t)$ exceeds $r(t)$, which results in a failure state. The limit state of the structure is that, the load process $S(t)$ does not exceed $r(t)$ at any time within the considered interval $[0, t_l]$. With this, the time-dependent reliability, $\mathrm{Rel}(t_l)$, is evaluated as follows,

$$\mathrm{Rel}(t_l) = \Pr(r(t) \geq S(t),\ \forall t \in [0, t_l]) \tag{1}$$

in which Pr( ) denotes the probability of the event in the brackets. Based on Eq. (1), the failure probability, $p_f(t_l)$, is evaluated by $p_f(t_l) = 1 - \mathrm{Rel}(t_l) = \Pr(r(t) < S(t),\ \exists t \in [0, t_l])$. Let $\nu^+(t)$ be the occurrence rate of upcrossings at time t, and $N(t_l)$ the number of upcrossings during $[0, t_l]$. For structures with a low probability of failure[2], the sequence of upcrossings can be described by a Poisson point process, with which the probability mass function (PMF) of $N(t_l)$ is as follows,

$$\Pr(N(t_l) = n) = \frac{1}{n!}\left\{\int_0^{t_l} \nu^+(t)dt\right\}^n \exp\left\{-\int_0^{t_l} \nu^+(t)dt\right\}, \quad n = 0, 1, 2, \ldots \tag{2}$$

[2] For example, if a structure is designed according to the ASCE standard 7–22 [22], the target reliability index has a typical range of 2.5–4.5 for a reference period of 50 years, yielding a failure probability between 3.4×10^{-6} and 6.2×10^{-3} over 50 years.

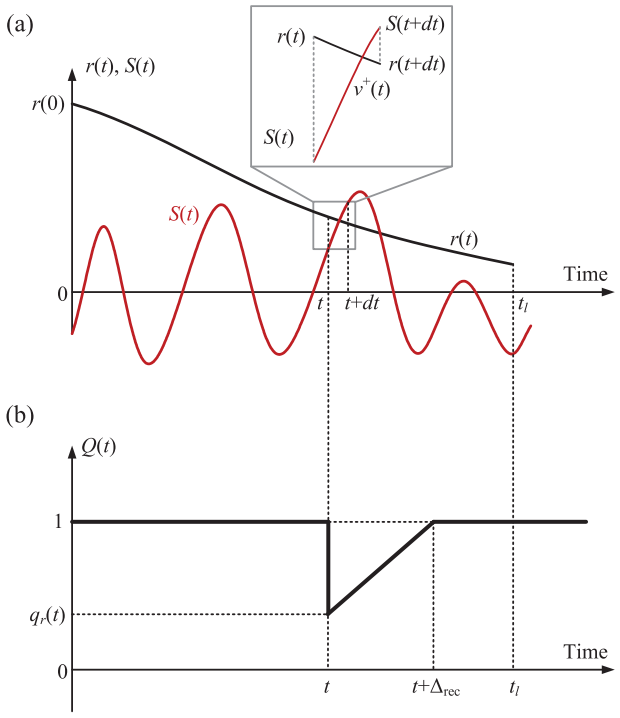

Fig. 1. Upcrossing-based reliability and resilience for a reference period of $[0, t_l]$. (a) Reliability. (b) Resilience.

Based on Eq. (2), the reliability over $[0, t_l]$ equals the probability of $N(t_l) = 0$ (i.e., no upcrossing occurs), with which

$$\mathrm{Rel}(t_l) = (1 - p_0) \cdot \exp\left\{-\int_0^{t_l} \nu^+(t)dt\right\} \tag{3}$$

where p_0 denotes the probability of failure at the initial time. Generally, one can treat the computation of p_0 as a time-invariant reliability problem, with which some well-established methods (e.g., first-order reliability method) are applicable. For specific cases where p_0 takes an extremely small value, and the structural failure is dominated by the resistance deterioration and/or nonstationary load effects, one can approximate Eq. (3) as follows,

$$\mathrm{Rel}(t_l) = \exp\left\{-\int_0^{t_l} \nu^+(t)dt\right\} \tag{4}$$

The expression for the upcrossing rate, $\nu^+(t)$, is evaluated as follows by referring to Fig. 1(a),

$$\begin{aligned}\lim_{dt\to 0} \nu^+(t)dt &= \Pr\left\{r(t) > S(t) \bigcap r(t+dt) < S(t+dt)\right\} \\ &= \int_{\dot{r}(t)}^{\infty} \left[\dot{S}(t) - \dot{r}(t)\right] f_{S\dot{S}}\left[r(t), \dot{S}(t)\right] d\dot{S}(t)dt\end{aligned} \tag{5}$$

where the dot over a variable refers to the derivative with respect to time, and $f_{S\dot{S}}$ is the joint probability density function (PDF) of $S(t)$ and $\dot{S}(t)$. Eq. (5) further yields the following (known as the Rice's formula [23]),

$$\nu^+(t) = \int_{\dot{r}(t)}^{\infty} \left(\dot{S}(t) - \dot{r}(t)\right) f_{S\dot{S}}\left(r(t), \dot{S}(t)\right) d\dot{S}(t) \tag{6}$$

In Eq. (6), if $S(t)$ a Gaussian process with a mean value of $\mu_S(t)$ and a standard deviation $\sigma_S(t)$ at time t, it follows that [15],

$$\begin{aligned}\nu^+(t) = \frac{\sigma_{\dot{S}|S}(t)}{\sigma_S(t)} \phi\left(\frac{r(t) - \mu_S(t)}{\sigma_S(t)}\right) \cdot \left[\phi\left(\frac{\dot{r}(t) - \mu_{\dot{S}|S}(t)}{\sigma_{\dot{S}|S}(t)}\right)\right. \\ \left. - \frac{\dot{r}(t) - \mu_{\dot{S}|S}(t)}{\sigma_{\dot{S}|S}(t)} \Phi\left(-\frac{\dot{r}(t) - \mu_{\dot{S}|S}(t)}{\sigma_{\dot{S}|S}(t)}\right)\right]\end{aligned} \tag{7}$$

where $\Phi(\,)$ and $\phi(\,)$ are the cumulative distribution function (CDF) and PDF of a standard normal distribution respectively, $\mu_S(t)$ and $\sigma_S(t)$ are the mean values and standard deviations of $S(t)$, $\mu_{\dot{S}|S}(t)$ and $\sigma_{\dot{S}|S}(t)$ are the conditional mean values and standard deviations of $\dot{S}(t)$ on $S(t)$, which are determined as follows,

$$\mu_{\dot{S}|S}(t) = \mu_{\dot{S}}(t) + \rho_{S\dot{S}}(t,t)\frac{\sigma_{\dot{S}}(t)}{\sigma_S(t)}[r(t) - \mu_S(t)] \tag{8}$$

$$\sigma_{\dot{S}|S}(t) = \sigma_{\dot{S}}(t) \cdot \sqrt{1 - \rho^2_{S\dot{S}}(t,t)} \tag{9}$$

where $\rho_{S\dot{S}}(t,t)$ is the correlation coefficient between the stochastic process $S(t)$ and its derivative $\dot{S}(t)$, and $\sigma_{\dot{S}}(t)$ is the standard deviation of $\dot{S}(t)$.

For a specific case where $S(t)$ has a time-invariant standard deviation of $\sigma_S(t) \equiv \sigma_S$, we introduce $S_0(t) = S(t) - \mu_S(t)$, which is a stationary Gaussian process with zero-mean and a constant standard deviation of σ_S. With this regard, let $\dot{S}_0(t)$ be the derivative of $S_0(t)$, which is statistically independent of $S_0(t)$, and has a time-invariant standard deviation of $\sigma_{\dot{S}}$. Focusing on an equivalent form of Eq. (1), $\mathrm{Rel}(t_l) = \Pr([r(t) - \mu_S(t)] \geq S_0(t),\ \forall t \in [0, t_l])$, Eq. (7) becomes

$$\begin{aligned}\nu^+(t) = \frac{\sigma_{\dot{S}}}{\sigma_S}\phi\left(\frac{r(t) - \mu_S(t)}{\sigma_S}\right) \cdot \left[\phi\left(\frac{\dot{r}(t) - \mu_{\dot{S}}(t)}{\sigma_{\dot{S}}}\right)\right. \\ \left. - \frac{\dot{r}(t) - \mu_{\dot{S}}(t)}{\sigma_{\dot{S}}}\Phi\left(-\frac{\dot{r}(t) - \mu_{\dot{S}}(t)}{\sigma_{\dot{S}}}\right)\right]\end{aligned} \tag{10}$$

Recall that Eq. (7) has been derived based on a Gaussian load process $S(t)$. For other types of load processes (e.g., a lognormal process), one can transform $S(t)$ into a Gaussian one, so that Eq. (7) applies. For example, based on the concept of Nataf transformation method [24–26], it follows that,

$$\Pr[r(t) - S(t) > 0] = \Pr\left\{\Phi^{-1}\left[F_{S(t)}(r(t))\right] - V(t) > 0\right\} \tag{11}$$

where $F_{S(t)}$ is the CDF of $S(t)$, and $V(t) = \Phi^{-1}\left[F_{S(t)}(S(t))\right]$. In such a way, the reliability problem is equivalent to that for a structure with a time-variant resistance of $\Phi^{-1}\left[F_{S(t)}(r(t))\right]$ subjected to a standard Gaussian load process $V(t)$ [16]. In this context, Eq. (7) becomes applicable.

Recall that in Eq. (4), a deterministic resistance has been considered (written as $r(t)$). If further taking into account the uncertainty associated with the resistance deterioration process, one can employ the law of total probability to modify the reliability method in Eq. (4). For instance, if the initial resistance, $R(0)$ is a random variable with a PDF of $f_{R(0)}(r)$ (note that $R(0)$ is involved in the expression of $\nu^+(t)$), the time-dependent reliability is evaluated as follows,

$$\mathrm{Rel}(t_l) = \int_0^\infty \exp\left\{-\int_0^{t_l} \nu^+(t)dt\right\} f_{R(0)}(r)dr \tag{12}$$

3. Proposed upcrossing-based model for time-dependent resilience

The aim of this section is to extend the existing method for time-dependent reliability to evaluate the time-dependent resilience of aging structures. As shown in Fig. 1(b), in the context of resilience, the emphasis is on the time-variation of the performance function, denoted by $Q(t)$, which takes a value between 0 and 1. For a reference period of $[0, t_l]$, the time-dependent resilience, $\mathrm{Res}(t_l)$, is evaluated based on $Q(t)$ as follows [27],

$$\mathrm{Res}(t_l) = \mu\left[\exp\left(\frac{1}{t_l}\int_0^{t_l} \ln Q(\tau)d\tau\right)\right] \tag{13}$$

in which $\mu(\,)$ denotes the mean value of the variable in the brackets. An accompanying item is called "nonresilience", which equals 1 minus resilience and may be used in some occasions for convenience.

Conditional on the occurrence of an upcrossing at time t, the structure suffers from a damage/failure state, resulting in the reduce of performance function from 1 (full serviceability) to a percentage $q_r(t) \in [0, 100\%]$, as shown in Fig. 1. This is followed by a recovery process of the performance function supported by the availability of resources. Note that $Q(t)$ is a stochastic process, given the uncertainties associated with the occurrence times of upcrossings, the recovery processes, and other factors. Thus, the resilience in Eq. (13) was assessed by taking the mean value of the right-hand part, yielding a scalar varying within [0,1]. Furthermore, it provides an efficient approach for resilience assessment if a closed form solution for Eq. (13) is available. This motivates the derivation of an explicit, upcrossing-based resilience method in the following.

3.1. Time-dependent resilience considering a survival-failure state

In this section, the resilience of a repairable structure over a service period of $[0, t_l]$ considering upcrossing-induced failure states is discussed. At time $t \in (0, t_l)$, due to the occurrence of an upcrossing, the structural performance degrades from 1 (full serviceability) to 0 as a result of the failure state (i.e., $q_r(t) = 0$ in Fig. 1), followed by an immediate recovery process of the performance function with a duration of Δ_{rec}. This accounts for the definition of a *repairable structure*, i.e., a structure that suffers from performance loss as a result of external attacks, and can be restored to the pre-hazard state via repair measures. Define

$$H(t) = \exp\left(\frac{1}{t_l}\int_t^{t+\Delta_{\mathrm{rec}}} \ln Q(\tau)d\tau\right) \tag{14}$$

which is a random variable due to the uncertainty associated with $Q(t)$. The mean value of $H(t)$ can be further evaluated explicitly based on the shape of the recovery profile. For example, with a linear recovery process, it follows that,

$$\begin{aligned}\mu(H(t)) &= \mu\left[\exp\left(\frac{1}{t_l}\int_t^{t+\Delta_{\mathrm{rec}}} \ln\left[\frac{1}{\Delta_{\mathrm{rec}}}(\tau - t)\right]d\tau\right)\right] \\ &= \mu\left[\exp\left(-\frac{\Delta_{\mathrm{rec}}}{t_l}\right)\right] = \int_0^\infty \exp(-x/t_l) f_{\Delta_{\mathrm{rec}}}(x)dx\end{aligned} \tag{15}$$

where $f_{\Delta_{\mathrm{rec}}}(x)$ is the PDF of Δ_{rec}, and x is the variable of integration. One can further extend Eq. (15) to fit other shapes of the recovery process.

For a reference period of $[0, t_l]$, the number of upcrossings is $N(t_l)$, whose PMF was shown in Eq. (2). If $N(t_l) = 0$, then $\mathrm{Res}(t_l) = 1$. Otherwise, conditional on $N(t_l) = n > 0$, let $\{T_1^*, T_2^*, \ldots T_n^*\}$ be the sequence of occurrence times of upcrossings, as shown in Fig. 2. Let $\Delta_{\mathrm{rec},i}$ be the duration of performance recovery associated with the ith upcrossing ($i = 1, 2, \ldots n$). Employing the Poisson process model for the time sequence, each T_i^* is statistically independent and identically distributed [6,28], with a common PDF (denoted by $f_{T^*}(t)$) as follows based on the upcrossing rate $\nu^+(t)$ in Eq. (7),

$$f_{T^*}(t) = \frac{\nu^+(t)}{\int_0^{t_l} \nu^+(\tau)d\tau}, \quad 0 \leq t \leq t_l \tag{16}$$

Assume that upon the occurrence of an upcrossing, the reduced performance function will be restored fully before the occurrence of the next upcrossing. There are different post-damage repair strategies to restore the structural performance [7], of which the "as-good-as-old" strategy will be considered in this paper. That is, the post-upcrossing structural resistance is repaired to the state as if the upcrossing did not occur. It is also assumed that the recovery profiles associated with different upcrossings are statistically independent, which is consistent with the "as-good-as-old" strategy, since the repair measures do not affect the subsequent occurrence of upcrossings. With this, the structural resilience over $[0, t_l]$, conditional on $N(t_l) = n$, is evaluated as follows for $n \geq 1$,

$$\begin{aligned}\mathrm{Res}(t_l)_{N(t_l)=n} &= \mu\left[\exp\left(\frac{1}{t_l}\sum_{i=1}^{n}\int_{T_i^*}^{T_i^*+\Delta_{\mathrm{rec},i}} \ln Q(\tau)d\tau\right)\right] \\ &= \prod_{i=1}^{n}\mu\left[\exp\left(\frac{1}{t_l}\int_{T_i^*}^{T_i^*+\Delta_{\mathrm{rec},i}} \ln Q(\tau)d\tau\right)\right] \\ &= \left(\int_0^{t_l} \mu(H(t)) \cdot f_{T^*}(t)dt\right)^n\end{aligned} \tag{17}$$

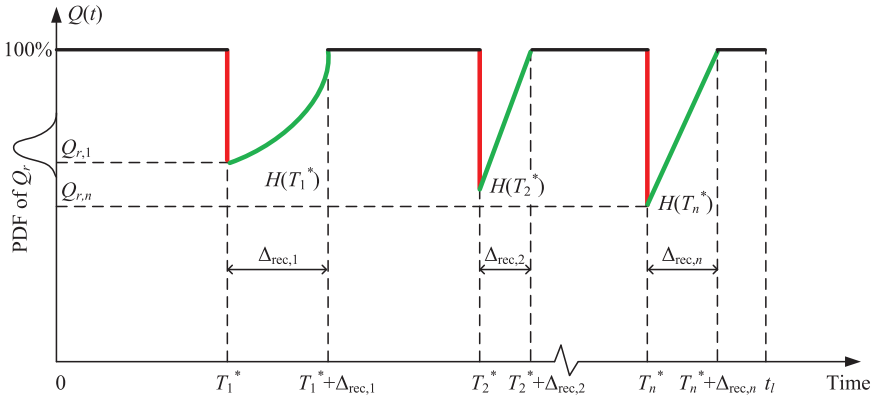

Fig. 2. Illustration of time-dependent resilience over a reference period of $[0, t_l]$.

The first line of Eq. (17) is explained by the fact that $Q(\tau) = 1$ for $\tau \notin [T_i^*, T_i^* + \Delta_{\text{rec},i}]$ (i.e., when the structure is not in a recovering state), with which $\ln Q(\tau) = 0$.

Note that Eq. (17) also holds for $n = 0$, although it has been derived for $n \geq 1$. Next, using the law of total probability, the unconditional resilience over $[0, t_l]$ is evaluated as follows,

$$\begin{aligned}\text{Res}(t_l) &= \sum_{n=0}^{\infty} \text{Res}(t_l)_{N(t_l)=n} \cdot \Pr(N(t_l) = n) \\ &= \exp\left\{-\int_0^{t_l} \nu^+(t)dt\right\} \cdot \sum_{n=0}^{\infty} \frac{1}{n!} \left\{\int_0^{t_l} \mu(H(t)) f_{T^*}(t)dt \cdot \int_0^{t_l} \nu^+(t)dt\right\}^n \\ &= \exp\left\{-\int_0^{t_l} \nu^+(t)dt\right\} \cdot \sum_{n=0}^{\infty} \frac{1}{n!} \left\{\int_0^{t_l} \mu(H(t))\nu^+(t)dt\right\}^n \\ &= \exp\left\{-\int_0^{t_l} \nu^+(t)[1 - \mu(H(t))]dt\right\}\end{aligned} \tag{18}$$

Eq. (18) presents the proposed resilience model for repairable structures over a reference period of $[0, t_l]$. In Eq. (18), based on the mean value theorem for integrals, there exists a time instant $t_0 \in [0, t_l]$ such that $\int_0^{t_l} \nu^+(t)[1 - \mu(H(t))]dt = [1 - \mu(H(t_0))] \int_0^{t_l} \nu^+(t)dt$, with which Eq. (18) becomes

$$\text{Res}(t_l) = \exp\left\{-[1 - \mu(H(t_0))] \int_0^{t_l} \nu^+(t)dt\right\} = \text{Rel}(t_l)^{1-\mu(H(t_0))} \tag{19}$$

in which $\text{Rel}(t_l)$ is the time-dependent reliability in Eq. (4). Eq. (19) reveals the inherent relationship between time-dependent reliability and resilience of aging structures. Since $0 \leq \mu(H(t_0)) \leq 1$, it follows that, $\text{Res}(t_l) \geq \text{Rel}(t_l)$, i.e., the reliability is a lower bound for resilience from a mathematical view. In particular, if $\mu(H(t_0)) = 0$ (e.g., there is no resource that supports the performance recovery), then the resilience reduces to reliability.

3.2. Time-dependent resilience considering multiple damage states

In Sect. 3.1, the resilience problem of repairable structures considering upcrossing-induced failure states has been addressed. This resilience model is extended herein to incorporate multiple damage states when an upcrossing occurs.

Conditional on the occurrence of an upcrossing, a structure may suffer from one of totally m damage states, denoted by DS1, DS2 through DSm respectively in an order of increasing severity, where m is a positive integer (Denote DS0 = no damage). These states are featured by m generalized capacities (GCs), denoted by $R_1, R_2, \ldots R_m$, whose CDFs take the same shapes as the fragility curves that define the multiple damage states [29–31]. Given a load effect s, the structure is in the DS0 state if $s < R_1$, suffers from DSi if $R_i \leq s < R_{i+1}$ for $i = 1, 2, \ldots m$, where $R_{m+1} = \infty$. It was proven in [30] that each GC is statistically fully correlated. A lognormal distribution shape is often assigned for the fragility curves [32,33], with which each GC is a lognormal variable. Let $\hat{R}_i$ and β_i be the median value and dispersion of R_i, respectively, for $i = 1, 2, \ldots m$. With this, the PDF of R_i, $f_{R_i}(x)$, takes a form of the following for any positive real number x,

$$f_{R_i}(x) = \frac{1}{\sqrt{2\pi} x \beta_i} \exp\left[-\frac{1}{2}\left(\frac{\ln x - \ln \hat{R}_i}{\beta_i}\right)^2\right] \tag{20}$$

Further, taking into account the deterioration processes of the GCs, reflecting the time-variation of the fragility curves [34], a deterioration function, $G_i(t)$, is introduced for the ith GC [31,35], i.e., $R_i(t) = R_i(0) \cdot G_i(t)$, where $R_i(t)$ is the ith GC evaluated at time t for $i = 1, 2, \ldots m$. The deterioration function is a stochastic process reflecting the uncertainty associated with the deterioration process of the fragility curves. One can determine $G_i(t)$ through fitting the fragility curves at discrete time instants (see, e.g., [31,35] for detailed discussions).

The resilience over $[0, t_l]$ conditional on $R_1(0) = r_1(0)$ is first derived, which will be later updated to incorporate the uncertainty associated with $R_1(0)$. Since each GC is fully correlated, one can uniquely determine $r_2(0)$ through $r_m(0)$ based on $r_1(0)$. Let $\nu_i^+(t)$ be the upcrossing rate of the load process $S(t)$ with respect to $r_i(t)$. It follows that,

$$\nu_1^+(t) > \nu_2^+(t) > \ldots > \nu_m^+(t) > \nu_{m+1}^+(t) \tag{21}$$

where $\nu_{m+1}^+(t) \equiv 0$ since $R_{m+1} = \infty$. For simplicity, an indicator for the damage state, $\mathcal{D}$, is introduced, taking a value of i for DSi, $i = 0, 1, 2, \ldots m$. Within a time interval of $[t, t + dt]$ with $dt \to 0$, one has,

$$\Pr(\mathcal{D} \geq i) = \nu_i^+(t) \cdot dt, \quad i = 1, 2, \ldots m \tag{22}$$

Note also that,

$$\begin{aligned}\Pr(\mathcal{D} \geq i) &= \Pr(\mathcal{D} \geq i \cap \mathcal{D} = i) + \Pr(\mathcal{D} \geq i \cap \mathcal{D} > i) \\ &= \Pr(\mathcal{D} = i) + \Pr(\mathcal{D} \geq i + 1)\end{aligned} \tag{23}$$

with which

$$\Pr(\mathcal{D} = i) = (\nu_i^+(t) - \nu_{i+1}^+(t)) \cdot dt = \theta_i(t) \cdot dt, \quad i = 1, 2, \ldots m \tag{24}$$

where $\theta_i(t) = \nu_i^+(t) - \nu_{i+1}^+(t)$ for $i = 1, 2, \ldots m$.

Let $N_i(t_l)$ be the number of upcrossings within $[0, t_l]$ that lead to DSi for $i = 1, 2, \ldots m$, which is a Poisson number with an occurrence rate of $\theta_i(t)$. Similar to Eq. (14), define

$$H_i(t) = \exp\left(\frac{1}{t_l} \int_t^{t+{}_i\Delta_{\text{rec}}} \ln Q_i(\tau)d\tau\right), \quad i = 1, 2, \ldots m \tag{25}$$

where ${}_i\Delta_{\text{rec}}$ is the duration of recovery process associated with DSi (this is not the same as $\Delta_{\text{rec},i}$ shown in Fig. 1(b)), and $Q_i(\tau)$ is the performance function during the recovery process associated with DSi.

Denote $\mathbf{N}(t_l) = \{N_1(t_l), N_2(t_l), \ldots N_m(t_l)\}$, and $\mathbf{n} = \{n_1, n_2, \ldots n_m\}$, where each n_i is a nonnegative integer for $i = 1, 2, \ldots m$. Motivated

by Eq. (17), the time-dependent resilience over $[0, t_l]$ conditional on $\mathbf{N}(t_l) = \mathbf{n}$ is evaluated as follows,

$$\mathrm{Res}(t_l)_{\mathbf{N}(t_l)=\mathbf{n}} = \prod_{i=1}^{m}\left(\int_0^{t_l} \mu(H_i(t)) \cdot \frac{\theta_i(t)}{\int_0^{t_l}\theta_i(\tau)d\tau} dt\right)^{n_i} \tag{26}$$

Further, based on the law of total probability, the unconditional resilience becomes,

$$\begin{aligned}\mathrm{Res}(t_l) &= \mu\left\{\prod_{i=1}^{m}\left(\int_0^{t_l} \mu(H_i(t)) \cdot \frac{\theta_i(t)}{\int_0^{t_l}\theta_i(\tau)d\tau} dt\right)^{N_i(t_l)}\right\} \\ &= \prod_{i=1}^{m}\left\{\sum_{n=0}^{\infty}\left(\int_0^{t_l} \mu(H_i(t)) \cdot \frac{\theta_i(t)}{\int_0^{t_l}\theta_i(\tau)d\tau} dt\right)^{n_i} \cdot \Pr(N_i(t_l) = n_i)\right\} \\ &= \prod_{i=1}^{m}\exp\left\{-\int_0^{t_l}\theta_i(t)[1-\mu(H_i(t))]dt\right\} \\ &= \exp\left\{-\int_0^{t_l}\sum_{i=1}^{m}\theta_i(t)[1-\mu(H_i(t))]dt\right\}\end{aligned} \tag{27}$$

If $m = 1$ in Eq. (27), then only a failure state is included, with which $\theta_1(t) = v_1^+(t)$, and Eq. (27) reduces to Eq. (18). With this regard, an alternative approach to obtaining Eq. (27) is to directly generalize Eq. (18), as detailed in Appendix A.

In Eq. (27), the resilience has been derived conditional on deterministic $R_1(0)$ and deterministic deterioration processes of GCs. Further, one can incorporate the uncertainty associated with $R_1(0)$ (or equivalently, $R_2(0)$ through $R_m(0)$) and each $G_i(t)$ in resilience assessment by using the law of total probability. For example, if each $G_i(t)$ takes a common form of $G_i(t) = 1 - Kt$, where K is a random variable reflecting the changing rate of the GCs, Eq. (27) becomes,

$$\mathrm{Res}(t_l) = \int_0^{\infty}\int_0^{\infty}\exp\left\{-\int_0^{t_l}\sum_{i=1}^{m}\theta_i(t)[1-\mu(H_i(t))]dt\right\} f_{R_1(0)}(r) f_K(k) dr dk \tag{28}$$

in which $f_{R_1(0)}(r)$ is the PDF of $R_1(0)$, $f_K(k)$ is the PDF of K and $\mu(H_i(t))$ is conditioned on $R_1(0) = r_1(0)$ and $K = k$.

4. Example

In this section, a numerical example is presented to demonstrate the applicability of the proposed resilience model in Eq. (28). Consider the resilience of a residential building over a reference period of 50 years subjected to wind load. The building has a gable roof archetype, with a roof slope 26.5° and a floor-to-area ratio of 0.1. Totally three damage states are considered for the building, namely moderate, extensive and collapse. These states are featured by three lognormally-distributed GCs, whose properties are adopted from [36] and are listed in Table 1. Taking into account the aging effects, assume that the median values of these GCs degrade by 20% linearly over 50 years. The load process (wind load), $S(t)$, is modeled by a Gaussian stochastic process with a mean value of $9(1 + \kappa t)$ m/s, and a constant standard deviation of 6 m/s. Here, t is time in year, and κ is a rate parameter. For example, if $\kappa = 0.004$, then the mean wind speed increases by 20% over 50 years, as will be used in the following analyses. While it is out of the scope of this paper to develop quantitative models for load nonstationarity, the load models used herein are representative of potential scenarios of future hazards.

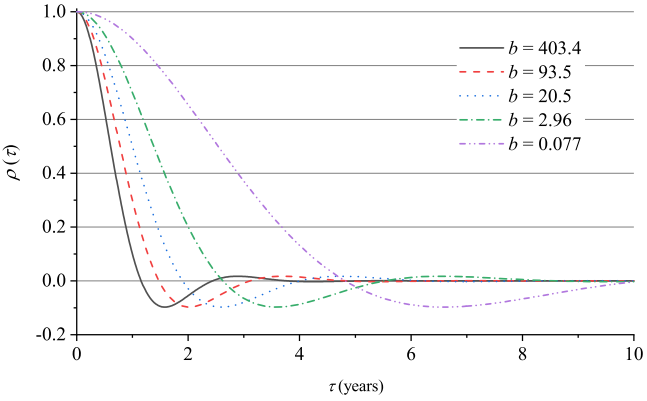

Fig. 3. The correlation function $\rho(\tau)$ of wind stochastic process.

The power spectral density function of the wind process, denoted by $S(\omega)$, takes a form of the following [16],

$$\mathcal{J}(\omega) \propto \frac{1}{\omega^6 + b}, \quad \omega \in (-\infty, \infty) \tag{29}$$

where b is a constant to be determined based on the correlation structure of the stochastic process as follows,

$$\rho(\tau) = \frac{1}{2}\exp\left(-\frac{b^{1/6}\tau}{2}\right)\cdot\left[\exp\left(-\frac{b^{1/6}\tau}{2}\right) + 2\cos\left(\frac{\sqrt{3}}{2}b^{1/6}\tau - \frac{\pi}{3}\right)\right] \tag{30}$$

where $\rho(\tau)$ is the correlation coefficient of the load process evaluated at two instances with a separation of τ. Fig. 3 illustrates the graph of $\rho(\tau)$, from which the value of b can be found via $\rho(1)$. For example, if $\rho(1) = 0.5$, then $b = 20.5$ (this value will be used in the following unless otherwise stated). With this, Eq. (10) applies, and it follows that,

$$\sigma_S(t) = \frac{1}{\sqrt{2}}b^{1/6}\sigma_S(t) \tag{31}$$

The mean values of the remaining performances and recovery durations associated with different damage states, as adopted from [37], are shown in Table 1. For illustration purpose, assume that the remaining performance follows a Beta distribution (as it varies within [0,1]) with a coefficient of variation (COV) of 0.1. The recovery time follows a Gamma distribution (for nonnegative random variables) with a COV of 0.2 and a linear shape of recovery. With this, one can readily evaluate $H_i(t)$ (defined in Eq. (25)) associated with these damage states, denoted by $H_1(t)$, $H_2(t)$ and $H_3(t)$. In this example, each $H_i(t)$ is time-invariant but is a function of t_l. For $H_1(t)$ and $H_2(t)$, one has,

$$\begin{aligned}\mu(H_i(t)) &= \int\int \exp\left(\frac{1}{t_l}\int_0^{\delta}\ln\left[q + \frac{1-q}{\delta}t\right]dt\right) f_{{}_iQ_r}(q) f_{{}_i\Delta_{\mathrm{rec}}}(\delta) dq d\delta \\ &= \int\int \exp\left[\frac{\delta}{t_l}\left(\frac{q\ln q}{q-1} - 1\right)\right] f_{{}_iQ_r}(q) f_{{}_i\Delta_{\mathrm{rec}}}(\delta) dq d\delta\end{aligned} \tag{32}$$

where $i = 1, 2$, ${}_iQ_r$ and ${}_i\Delta_{\mathrm{rec}}$ are the remaining performance and recovery time associated with DSi, $f_{{}_iQ_r}(q)$ and $f_{{}_i\Delta_{\mathrm{rec}}}(\delta)$ are the PDFs of ${}_iQ_r$ and ${}_i\Delta_{\mathrm{rec}}$, respectively. Note that Eq. (32) is consistent with Eq. (15) since

$$\lim_{q\to 0}\frac{q\ln q}{q-1} = 0 \tag{33}$$

However, for the "collapse" damage state, there is no resource that supports the recovery process of performance, with which $H_3(t) = 0$.

Table 1
Wind-resisting capacity and post-hazard performance of a residential building.

Damage state	Median of GC (m/s)	Dispersion of GC	Expected remaining performance	Expected recovery time (days)
Moderate	22.87	0.09	90%	120
Extensive	31.50	0.05	50%	360
Collapse	41.26	0.04	0%	/

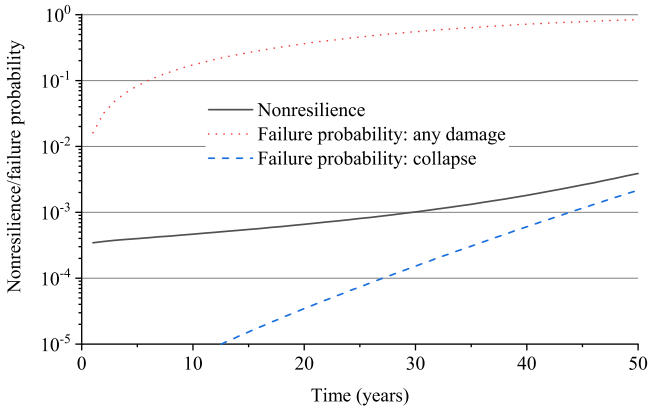

Fig. 4. Time-dependent nonresilience/failure probability for reference periods up to 50 years.

Fig. 4 shows the time-dependent resiliences of the residential building for reference periods up to 50 years, as calculated by Eq. (28). For comparison purpose, the time-dependent failure probabilities associated with two limit state functions are also plotted in Fig. 4: (1) the occurrence of any damage (either moderate, extensive or collapse), and (2) the occurrence of collapse. The nonresilience/failure probability increases with time, reflecting the accumulation of risks over time. The failure probability associated with the occurrence of any damage is greater than the nonresilience, which is consistent with the observation from Eq. (19). However, the failure probability related to the collapse state is a lower bound for nonresilience. This is explained from a mathematical perspective by the fact that,

$$\theta_3(t) < \sum_{i=1}^{3} \theta_i(t)[1-\mu(H_i(t))] < \sum_{i=1}^{3} \theta_i(t) \tag{34}$$

which further yields,

$$1-\exp\left(-\int_0^{t_l} \theta_3(t)dt\right) < 1-\exp\left(-\int_0^{t_l} \sum_{i=1}^{3} \theta_i(t)[1-\mu(H_i(t))]dt\right) < 1-\exp\left(-\int_0^{t_l} \sum_{i=1}^{3} \theta_i(t)dt\right) \tag{35}$$

In Fig. 5(a), the role of correlation of the load process in resilience is investigated, considering different values of $\rho(1)$ in Eq. (30). The case of stronger correlation in load results in smaller nonresilience. For example, for a service life of 50 years, the nonresilience equals 6.3×10^{-3} with $\rho(1) = 0.1$, which becomes 1.6×10^{-3} if $\rho(1) = 0.9$. This difference is due to the weakened wind risks in the presence of stronger wind correlation. To demonstrate this point, examining the CDF of the maximum wind speed over 50 years as illustrated in Fig. 5(b), it is found that, with a greater value of $\rho(1)$, the CDF shifts towards left, leading to a lower probability of extreme wind speed at the upper tail.

The impact of wind nonstationarity on resilience is examined in Fig. 6(a), based on different increasing scenarios of the mean wind speed over 50 years. A more severe increase in wind load results in greater nonresilience. For example, with $t_l = 50$ years, the nonresilience equals 1.9×10^{-3} in the presence of a stationary load process, which becomes 4.2 times if the mean value of wind speed increases by 40% over 50 years. The comparison between the different curves in Fig. 6(a) demonstrates the importance of properly projecting the future wind scenarios in a changing climate when evaluating structural time-dependent resilience. In Fig. 6(b), the effect of GC deterioration on resilience is shown with varying deterioration scenarios over 50 years (the values in the legends refer to the variation of GC median). The nonresilience is significantly amplified with a more severe deterioration of the GCs. For instance, for a service period of 50 years, the nonresilience associated with a deterioration scenario of 40% over 50 years is 171 times that associated with time-invariant GCs. The comparison between Fig. 6(a) and (b) implies that the nonresilience is more sensitive to the variation of GC deterioration.

5. Concluding remarks

In this paper, a new method for the assessment of time-dependent resilience of aging structures has been proposed. Modeling the load process as a continuous stochastic process, an upcrossing is deemed to occur when the load effect exceeds the resistance/capacity, which leads to the reduction of performance function. The proposed method can take into account upcrossing-induced multiple damage states, and evaluates the resilience with a closed form solution. An example has been presented in this paper to demonstrate the applicability of the proposed resilience model considering wind hazards. The following conclusions can be drawn from this paper.

1. The time-dependent resilience can be treated as a generalized form of time-dependent reliability from a mathematical view, if not taking into account the post-damage recovery process of performance. This provides insights into the inherent relationship between the two important quantities – reliability and resilience.

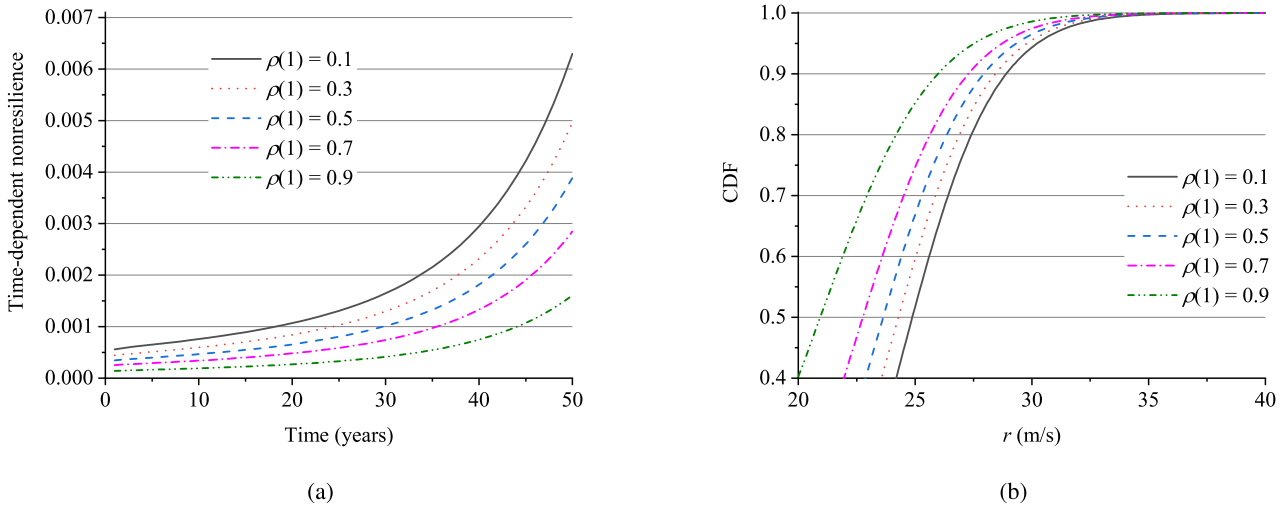

Fig. 5. Impact of correlation of wind stochastic process on resilience. (a) Time-dependent nonresilience. (b) CDF of maximum wind speed over 50 years.

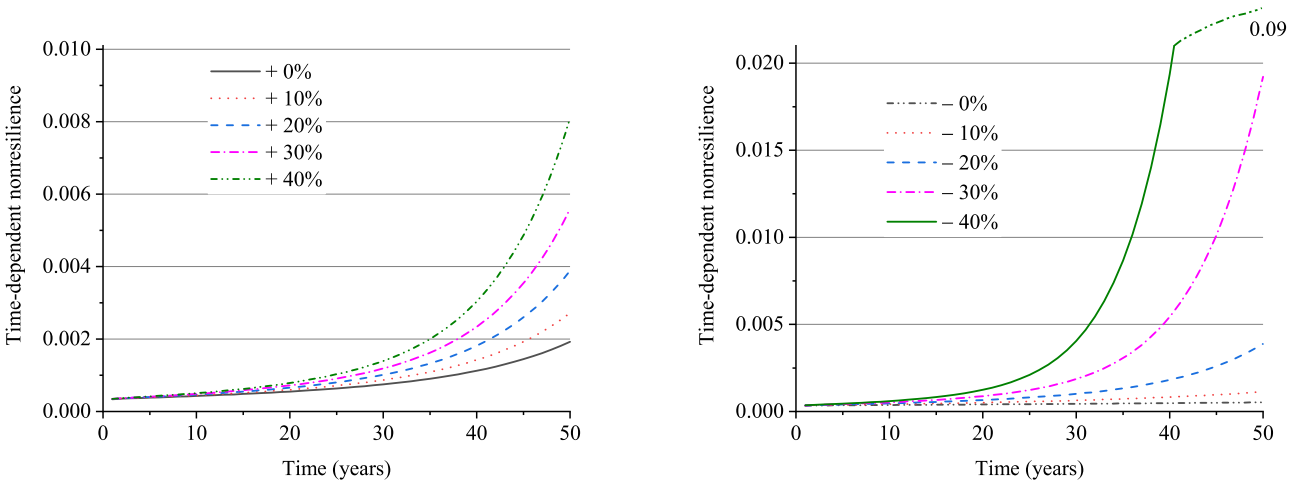

(a) Effect of wind nonstationarity (b) Effect of GC deterioration

Fig. 6. Effects of wind process and GC deterioration on resilience.

2. It is an important ingredient to capture the correlation structure of the load process in resilience assessment. In the presence of stronger correlation in load, the nonresilience becomes smaller, due to the weakened risks to the structure.
3. Ignoring the potential impacts of climate change will underestimate the nonresilience, yielding a relatively non-conservative evaluation. For a reference period of 50 years, the structural nonresilience considering an increase in mean wind speed of 40% over 50 years is 4.2 times that associated with a stationary wind process. This implies the importance of reasonable projection of future load effects for use in resilience analysis.

Relevance to resilience

A new method is developed to evaluate the time-dependent resilience of aging structures subjected to a continuous load process. The proposed method takes into account the aging effects of the structural resistance/capacity and the nonstationarity in loads.

Declaration of competing interest

The author declares that he has no known competing financial interests or personal relationships that could have appeared to influence the work reported in this paper.

CRediT authorship contribution statement

Cao Wang: Conceptualization, Data curation, Formal analysis, Funding acquisition, Investigation, Methodology, Project administration, Resources, Software, Supervision, Validation, Visualization, Writing – original draft, Writing – review & editing.

Acknowledgements

This research described in this paper was supported by the Australian Government through the Australian Research Council's Discovery Early Career Researcher Award (DE240100207). This support is gratefully acknowledged. The views expressed herein are those of the author and are not necessarily those of the Australian Government or Australian Research Council.

Appendix A. An alternative approach to deriving Eq. (27)

In this section, an alternative approach to deriving Eq. (27) is presented. Note that,

$$\Pr(D=i|D\geq 1)=\frac{\Pr(D=i)}{\Pr(D\geq 1)}=\frac{\theta_i(t)}{\nu_1^+(t)} \tag{A.1}$$

The resilience model in Eq. (18) is used herein by replacing $\nu^+(t)$ with $\nu_1^+(t)$. In the context of considering m damage states, the item $\mu(H(t))$ in Eq. (18) is revised as follows by using the law of total probability,

$$\begin{aligned}\mu(H(t)) &= \sum_{i=1}^{m}\mu(H_i(t))\cdot\Pr(D=i|D\geq 1)\\ &= \sum_{i=1}^{m}\mu(H_i(t))\cdot\frac{\theta_i(t)}{\nu_1^+(t)}\end{aligned} \tag{A.2}$$

Substituting Eq. (A.2) into Eq. (18), it follows that,

$$\begin{aligned}\mathrm{Res}(t_l) &= \exp\left\{-\int_0^{t_l}\nu_1^+(t)\left[1-\sum_{i=1}^{m}\mu(H_i(t))\cdot\frac{\theta_i(t)}{\nu_1^+(t)}\right]dt\right\}\\ &= \exp\left\{-\int_0^{t_l}\nu_1^+(t)dt+\int_0^{t_l}\sum_{i=1}^{m}\theta_i(t)\cdot\mu(H_i(t))dt\right\}\end{aligned} \tag{A.3}$$

Further, note that

$$\nu_1^+(t)=\sum_{i=1}^{m}\theta_i(t) \tag{A.4}$$

with which Eq. (A.3) becomes Eq. (27).

Appendix B. Modified version of Eq. (27) considering the gradual deterioration of performance

Recall that in Eqs. (18) and (27), it has been assumed the performance function $Q(t)$ is independent of the deterioration process of resistance $R(t)$. Herein, the resilience model in Eq. (27) is modified by incorporating the impact of gradual deterioration of performance (note that Eq. (18) is a specific case of (27)).

Denote $q(t)$ the time-variant performance at time t, and define $\widetilde{Q}(t)=Q(t)/q(t)$. With this, Eq. (13) becomes the following,

$$\begin{aligned}\mathrm{Res}(t_l) &= \mu\left[\exp\left(\frac{1}{t_l}\int_0^{t_l}\ln[q(\tau)\cdot\widetilde{Q}(\tau)]d\tau\right)\right]\\ &= \exp\left(\frac{1}{t_l}\int_0^{t_l}\ln q(\tau)d\tau\right)\cdot\mu\left[\exp\left(\frac{1}{t_l}\int_0^{t_l}\ln\widetilde{Q}(\tau)d\tau\right)\right]\end{aligned} \tag{B.1}$$

Similar to Eq. (25), define

$$\widetilde{H}_i(t) = \exp\left(\frac{1}{t_l}\int_t^{t+{}_i\Delta_{\text{rec}}} \ln \widetilde{Q}_i(\tau)d\tau\right), \quad i = 1, 2, \dots m \tag{B.2}$$

in which $\widetilde{Q}_i(\tau) = Q_i(\tau)/q(\tau)$. With this, based on Eq. (27), Eq. (B.1) becomes,

$$\text{Res}(t_l) = \exp\left(\frac{1}{t_l}\int_0^{t_l} \ln q(\tau)d\tau\right)\cdot \exp\left\{-\int_0^{t_l}\sum_{i=1}^{m}\theta_i(t)\left[1-\mu\left(\widetilde{H}_i(t)\right)\right]dt\right\} \tag{B.3}$$

Eq. (B.3) presents a model for the time-dependent resilience considering the gradual deterioration of performance, reflected through the item $q(\tau)$. In particular, if $q(\tau) \equiv 1$, then Eq. (B.3) reduces to Eq. (27).

References

[1] Ellingwood BR, Mori Y. Reliability-based service life assessment of concrete structures in nuclear power plants: optimum inspection and repair. Nucl Eng Des 1997;175(3):247–58.
[2] Alipour A, Shafei B, Shinozuka M. Performance evaluation of deteriorating highway bridges located in high seismic areas. J Bridge Eng 2011;16(5):597–611.
[3] Edirisinghe R, Setunge S, Zhang G. Application of gamma process for building deterioration prediction. J Perform Constr Facil 2013;27(6):763–73.
[4] Wang C. A stochastic process model for resistance deterioration of aging bridges. Adv Bridge Eng 2020;1(1):3.
[5] Ellingwood BR. Risk-informed condition assessment of civil infrastructure: state of practice and research issues. Struct Infrastruct Eng 2005;1(1):7–18.
[6] Wang C. Structural reliability and time-dependent reliability. Springer Cham; 2021.
[7] Ayyub BM. Systems resilience for multihazard environments: Definition, metrics, and valuation for decision making. Risk Anal 2014;34(2):340–55.
[8] Bruneau M, Reinhorn A. Exploring the concept of seismic resilience for acute care facilities. Earthq Spectra 2007;23(1):41–62.
[9] Basu AK. Introduction to stochastic process. Alpha Science International Ltd; 2003.
[10] IPCC. Climate change 2021: The physical science basis. Contribution of working group i to the sixth assessment report of the intergovernmental panel on climate change. Cambridge University Press; 2021.
[11] Reguero BG, Losada InJ, Méndez FJ. A recent increase in global wave power as a consequence of oceanic warming. Nat Commun 2019;10(1):205.
[12] Toimil A, Losada InJ, Nicholls RJ, Dalrymple RA, Stive MJF. Addressing the challenges of climate change risks and adaptation in coastal areas: a review. Coastal Eng 2020;156:103611.
[13] Liu J, Li R, Li S, Meucci A, Young IR. Increasing wave power due to global climate change and intensification of antarctic oscillation. Appl Energy 2024;358:122572.
[14] Wang C-H, Wang X, Khoo YB. Extreme wind gust hazard in Australia and its sensitivity to climate change. Nat Hazards 2013;67:549–67.
[15] Li CQ, Melchers RE. Outcrossings from convex polyhedrons for nonstationary Gaussian processes. J Eng Mech 1993;119(11):2354–61.
[16] Wang C, Zhang H, Beer M. Structural time-dependent reliability assessment with new power spectral density function. J Struct Eng 2019;145(12):04019163.
[17] Yang W, Zhang B, Wang W, Li C-Q. Time-dependent structural reliability under non-stationary and non-Gaussian processes. Struct Saf 2023;100:102286.
[18] Yang DY, Frangopol DM. Life-cycle management of deteriorating civil infrastructure considering resilience to lifetime hazards: a general approach based on renewal-reward processes. Reliab Eng Syst Saf 2019;183:197–212.
[19] Wang C, Ayyub BM. Time-dependent resilience of repairable structures subjected to nonstationary load and deterioration for analysis and design. ASCE-ASME J Risk Uncertainty Eng Syst Part A Civ Eng 2022;8(3):04022021.
[20] Wang C, Ayyub BM. Time-dependent seismic resilience of aging repairable structures considering multiple damage states. Earthq Eng Resilience 2022;1(1):73–87.
[21] Mori Y, Ellingwood BR. Reliability-based service-life assessment of aging concrete structures. J Struct Eng 1993;119(5):1600–21.
[22] 7-22 A. Minimum design loads for buildings and other structures. Reston, Virginia: American Society of Civil Engineers; 2022.
[23] Rice SO. Mathematical analysis of random noise. Bell Syst Tech J 1944;23(3):282–332.
[24] Grigoriu M. Crossings of non-Gaussian translation processes. J Eng Mech 1984;110(4):610–20.
[25] Zheng R, Ellingwood BR. Stochastic fatigue crack growth in steel structures subject to random loading. Struct Saf 1998;20(4):303–23.
[26] Kim H, Shields MD. Modeling strongly non-Gaussian non-stationary stochastic processes using the iterative translation approximation method and Karhunen–Loève expansion. Comput Struct 2015;161:31–42.
[27] Wang C. A generalized index for functionality-sensitive resilience quantification. Resilient Cities Struct. 2023;2(1):68–75.
[28] Taylor HM, Karlin S. An introduction to stochastic modeling. 3rd ed. Academic Press; 1998. ISBN 978-0-12-684887-8
[29] Baker JW. Introducing correlation among fragility functions for multiple components. In: Proceedings of the 14th World conference on earthquake engineering, October 12–17, 2008, Beijing, China; 2008.
[30] Wang C, Zhang H, Ellingwood BR, Guo Y, Mahmoud H, Li Q. Assessing post-hazard damage costs to a community's residential buildings exposed to tropical cyclones. Struct Infrastruct Eng 2020;17(4):443–53.
[31] Wang C, Zhang H. Assessing the seismic resilience of power grid systems considering the component deterioration and correlation. ASCE-ASME J Risk Uncertain Eng Syst Part B Mech Eng 2020;6(2):020903.
[32] Cornell CA, Jalayer F, Hamburger RO, Foutch DA. Probabilistic basis for 2000 SAC federal emergency management agency steel moment frame guidelines. J Struct Eng 2002;128(4):526–33.
[33] Li Y, Ellingwood BR. Hurricane damage to residential construction in the US: importance of uncertainty modeling in risk assessment. Eng Struct 2006;28(7):1009–18.
[34] Ghosh J, Padgett JE. Aging considerations in the development of time-dependent seismic fragility curves. J Struct Eng 2010;136(12):1497–511.
[35] Wang C, Teh LH. Time-dependent seismic reliability of aging structures. ASCE-ASME J Risk Uncertainty Eng Syst Part A Civ Eng 2022;8(2):04022010.
[36] Abdelhady AU, Spence SMJ, McCormick J. Risk and fragility assessment of residential wooden buildings subject to hurricane winds. Struct Saf 2022;94:102137.
[37] FEMA. Multi–hazard loss estimation methodology: hurricane model. Washington, DC: Department of Homeland Security, Federal Emergency Management Agency, Mitigation Division; 2003.